

RSC Advances



This is an *Accepted Manuscript*, which has been through the Royal Society of Chemistry peer review process and has been accepted for publication.

Accepted Manuscripts are published online shortly after acceptance, before technical editing, formatting and proof reading. Using this free service, authors can make their results available to the community, in citable form, before we publish the edited article. This *Accepted Manuscript* will be replaced by the edited, formatted and paginated article as soon as this is available.

You can find more information about *Accepted Manuscripts* in the [Information for Authors](#).

Please note that technical editing may introduce minor changes to the text and/or graphics, which may alter content. The journal's standard [Terms & Conditions](#) and the [Ethical guidelines](#) still apply. In no event shall the Royal Society of Chemistry be held responsible for any errors or omissions in this *Accepted Manuscript* or any consequences arising from the use of any information it contains.

Tweaking Anisotropic Gold Nanostars: Covariant control of Polymer-solvent mixture complex

Abhitosh Kedia, Harsh Kumar and Pandian Senthil Kumar¹

Department of Physics & Astrophysics, University of Delhi, Delhi 110007 INDIA

Binary solvent mixture (N,N-Dimethylformamide (DMF):Propanol in the present case) solely has been employed for the first time in a simple yet versatile approach for the *in situ* intuitive and highly tweaked formation of the complex anisotropic gold nanostructures. In this novel approach, the uncommon usage of the polar/non-polar binary solvent mixture provides extra degrees of freedom in tailoring the intrinsic solution properties via simultaneously modified dipole-dipole/H-bonding interaction with the universally soluble amphiphilic polymer PVP, as carefully monitored through NMR, which further establishes a rational paradigm in better understanding the kinetic control over both nucleation as well as size/shape transition/evolution of reproducible anisotropic Au nanostructure morphology, as consistently revealed/correlated through optical absorption and TEM measurements respectively. Such kind of unusual size/shape transformation strategy of gold nanostructures yielding precise tuning of their respective plasmonic characteristics over the entire visible/NIR spectral range, significantly enables them to serve as excellent candidates/substrates for tunable surface enhanced Raman spectroscopy (SERS), the preliminary measurements of which are systematically illustrated.

¹ Corresponding Author
Email: pskumar@physics.du.ac.in

Introduction

Owing to the highly specific size/shape dependent physico-chemical properties of metal nanoparticles (NPs) such as their localized surface plasmon resonance (SPR) or high catalytic activity,¹⁻⁷ relentless extra care needs to be taken in stabilizing/tweaking the aesthetics of the asymmetric metal NPs with complex morphologies (such as polyhedra, multipods, star/flower etc.).⁸⁻¹⁹ Till now, vast number of literature reports are available on the tweaking/shaping of controlled gold nanostructures (with/without seed mediation) utilizing routinely a variety of surfactants/polymers like CTAB/PVP/ 2-[4-(2-hydroxyethyl)-1-piperazine]ethane-sulfonic acid (HEPES) etc., as shape directing/stabilizing agents.^{8-11, 15-17, 20} In some selective reports, alternative approaches, such as the gradual size tuning of the citrate reduced Au nanospheres via change in Cl⁻ ion concentration in solution,²¹ or synthesis of multiple shaped Au by different dendritic peptides,²² or precise control of size and nanostructuration of multi-branched of Au NPs by changing the HEPES concentration,^{20,23} and very recently tuning the plasmonic response of Au nanostar arrays from visible to near infrared by electron beam lithography,²⁴ have also been demonstrated. Understanding the morphological transition mechanism in noble metal NPs becomes an inevitable tool for not only engineering their plasmonic response from visible to far IR region of the EM spectrum,¹⁹⁻²⁸ but also for extending their application potentials from plasmonics to nanophotonics to biosensing and SERS etc.¹⁻⁵

So far, most of the successful colloidal synthetic procedures for the production of monodisperse/uniform colloidal gold nanoparticles utilize aqueous medium but synthetic schemes in organic media have also been reported recently.¹⁰⁻¹⁸ Among which DMF, a

well known polar aprotic organic solvent for its high synthetic value, good chemical and thermal stability (even at its boiling point, 153.8⁰C) has been widely chosen for the preparation of anisotropic gold nanostructures with a variety of geometrical shapes.^{16,18,29-}

³⁰ In conjunction with PVP, the high polar DMF solvent has been successfully utilized in tweaking/morphological transition the size/shape of complex 3D gold nanostars in a controlled manner using the well known seed mediated synthesis by varying size/concentration of the seed particle in the growth solution,³¹⁻³² which induces changes in the core size, the number, length and broadening of the branches. These gold nanostructures extend their plasmonic response well towards the near IR region due to the presence of sharp edges/tips, where strong localization of electromagnetic field exists, suggesting strong application potentials in the field of nanoantennas and nanophotonics.³³⁻³⁴ The nanoscale control of surface roughness/branching, ranging from planar anisotropic to complex elongated spikes, allows precise tuning of the nanoparticle optical properties with a high level of accuracy. Such anisotropic nanostructures were demonstrated to be excellent candidates for SERS applications.³⁵⁻³⁹

In our previous reports, we have already discussed in detail that increasing the pH of the reaction mixture conveniently results in fine tuning of the plasmon band as well as the morphology of gold nanostars in a single step synthetic protocol.²⁸ Furthermore, the solvent interaction with PVP, which has been reiterated as a crucial factor,¹⁷ wherein we illustrate that the solvent-solute interaction dominates the nucleation regime in precise and additionally plays a significant role in the polymer chemisorption onto the surface of the metal nanoparticles directing/shaping them to anisotropically grow with different intriguing size/shapes.

Convinced by the fact that the conformational changes of PVP in different solvents lead to different size/shaped Au nanostructures¹⁷ and in terms of simplifying the two-step seed mediated synthesis procedures for tuning the metal nanostructure morphology,^{31-32, 40} herein, we utilized a novel versatile single step synthesis protocol, involving the use of binary solvent mixture, such as DMF:2-propanol, for the first time to the best of our knowledge, resulting in the sequential tuning of gold nanostars, in sharp contrast with the formation of regular structures such as the nanocubes⁴¹ and nanowires⁴² as reported earlier. The good donor/acceptor properties of DMF enable it to dissolve a wide range of polar/non-polar solvents and its physico-chemical properties were studied in detail in conjunction with various solvents like water, alcohol etc., where the nature of molecular interaction between DMF and other solvents were carefully discussed in detail.⁴³⁻⁴⁷ The introduction of 2-propanol into DMF changes its H-bonding tendency as well as the dipole-dipole interaction, which plays a crucial role in governing the conformational changes of PVP, thus determining its reducing ability, thereby providing the necessary extra degrees of freedom for the controlled tuning of the plasmonic response of gold nanostars in a sequential manner from visible to the near IR region and can be used for specific applications such as the surface enhancement Raman scattering (SERS).

Materials and Methods

In a typical synthesis, 24 μ l aqueous solution of Hydrochloroauric acid ($\text{HAuCl}_4 \cdot 3\text{H}_2\text{O}$, Aldrich) of concentration 0.17 M was mixed homogeneously with 10 mM Polyvinylpyrrolidone (PVP average MW=10000, Aldrich) solution in 15 ml Dimethylformamide (DMF, Merck) and continuously stirred respectively in order to obtain gold nanostars in seedless colloidal synthesis procedure. Further detailed

synthesis procedure and mechanism of the formation of gold nanostars is discussed in our previous work,¹⁸ except that in the present work, the influence of 2-propanol is studied by adding it into DMF in different molar ratio before the addition of PVP and metal precursor. The molar ratio of PVP to metal ions (calculated in terms of polymer repeating unit or monomer chain length) is kept at ~ 3250 in all our experimental conditions. Change in color of solutions indicate the formation of gold nanostructures. All experiments and the various sample preparation procedures were carried out at room temperature, unless otherwise mentioned. Henceforth, 2-propanol will be referred as propanol.

Optical absorption measurements were recorded in all our as-prepared nanoparticle solution samples in the wavelength range of 200-1100 nm using Thermo Scientific absorption spectrophotometer. The ^{13}C NMR spectra were recorded on Bruker Avance-400 spectrometer using TMS as internal standard and CDCl_3 as a NMR solvent (chemical shifts in ppm). TEM samples were prepared by drying the five-fold centrifuged samples in ethanol at around 4500 rpm (to remove excess PVP) on carbon formvar coated copper grids and the images were acquired using FEI-Technai G^2 system operated at an accelerating voltage of 300 kV. The surface enhanced Raman scattering (SERS) spectra were obtained using a Renishaw inVia Raman Spectrometer with 785 nm He-Ne laser source. Samples for SERS were prepared by five-fold centrifuged Au nanoparticles dispersed in chloroform which were spread to form a monolayer at the air-water interface and is lifted onto the silicon substrates followed by the drop-cast deposition of the 10^{-6} M of the dye molecule, crystal violet. The SERS spectra were obtained for two different position of each of the samples and plotted on average.

Results and Discussion

Figure 1 shows the ^{13}C NMR spectra of DMF and propanol at different mole fraction (MF) of DMF with respect to propanol concentration. At high MF of DMF i.e., at low concentration of propanol in DMF, the ^{13}C carbonyl chemical shift of DMF increases slightly (see figure 1 for peak values) signifying the changes occurring in the self-association equilibria of DMF, which are evidently due to the change in dipole-dipole interaction along with the formation of hydrogen bonds, O–H (of propanol)...N(CH₃)₂ or O=CN of DMF along with H-bonding between H-O of propanol and the formyl proton of DMF as schematically shown in the scheme 1. With further decrease in the MF of DMF, the ^{13}C carbonyl chemical shift of DMF increases more rapidly (see figure 1 for peak values), demonstrating the fact that DMF-propanol hydrogen bonding increases with increasing alcohol content, and DMF is surrounded by more and more propanol molecules, similar to the case of DMF in methanol,⁴⁵ thereby visualizing propanol as a watermelon in which the DMF molecules act as seeds. The observed results indicate the existence of intermolecular association between O-H group of alcohol and C=O group of DMF along with DMF-DMF and alcohol-alcohol interactions as reported earlier as well.⁴⁷

Moreover, the interaction between PVP-DMF and PVP-propanol systems were individually discussed in detail in our previous work,¹⁷ which talks about the dominant dipole-dipole interaction in PVP-DMF system as well as the hydrophobic interaction between PVP and propanol. In the present case, PVP addition to the DMF/propanol composition (for different MF) results in the slow but steady re-organization of the polymer network, as systematically depicted in the scheme 2 in accordance with the ^{13}C

NMR studies (figure 2). A slight but sure downfield of the carbonyl peak (C=O peak around 175 ppm)⁴⁸ of PVP with decrease in MF of DMF (see figure 2 for peak values) signifies the weakening of H-bonding between DMF and propanol along with the appraisal of hydrophobic interaction between propanol and long chain of PVP molecules through hydrogen bond formation between nitrogen of PVP and HO-C of propanol as portrayed in scheme 2. The slight up-field chemical shift in the DMF carbonyl peak and the corresponding downfield shift in the C-OH bond of propanol (with increase in propanol volume) in the DMF-propanol-PVP system in comparison to DMF-propanol, exemplifies the loosening of DMF-PVP bonding in conjunction with increasing PVP-propanol H-bonding interaction with ostensibly augmenting the incremental increase in the hydrophobic interaction assimilated through the long polymer chain structure and the relatively smaller alcohol group and is maximum for pure PVP-propanol system.

In contrast, when HAuCl_4 is added to this PVP-binary solvent mixture, instantaneous solvation as well as the dynamically unstable PVP-AuCl_4^- complexation effectively takes place owing to the presence of lone pair of electrons in the oxygen as well as nitrogen atoms of the entangled PVP network, sequentially disproportionating itself to form Au^0 species in the absence of any other external reducing agent or energy resources. These in-situ formed tiny gold seed particles then compete with the polymer, PVP (the affinity of which decreases starting from DMF to propanol in the whole composition range used in the present case), thereby desolvating the surrounding DMF molecules in addition to weakening the PVP-propanol hydrogen bonding (as shown from the Au nanoparticles NMR, upfield chemical shifts of PVP, DMF and propanol carbonyl peaks in figure 3) in comparison to PVP-DMF-propanol mixture shown in figure 2. On the contrary, upon

addition of gold precursor to the PVP-propanol system, the observed slight downfield chemical shift of the PVP carbonyl peak (with respect to PVP-propanol, see figures 2 and 3) has been attributed to the fact that the hydrogen bonding between PVP and propanol remains almost intact and further dominated by strong hydrophobic interactions. This kind of composite reduction along with steric stabilization of PVP on the gold seed particles in the binary solvent system exclusively result in the steady/stable anisotropic nanoparticle growth, which has not been possible with any other conventional colloidal growth techniques.

Thus, the relevant stabilization of the as-prepared gold nanoparticle morphology has been coherently discussed utilizing transmission electron microscopy (TEM) in the light of distinct molecular interaction existing between DMF-propanol-PVP mixtures as discussed above.

In comparison with the gold nanostars synthesized in pure DMF, where the tips/spikes are longer and sharper, the sequential addition of propanol to DMF (decrease in MF of DMF) brought sequential changes in the sharpness, length and size of the tips/spikes as demonstrated clearly in figure 4. The proposed aperture angle α increases sequentially, signifying the size/shape poly-dispersion as well as the explicit broadening of tips/spike like features at the expense of their number density along with decrease in the overall size of the as-formed gold nanostructures, as clearly seen from the high magnification TEM images in figure 5b; further measurements under different TEM tilt angles would be of great interest in eliminating the so-called projection effect and for necessary quantification of the obtained data.

Such visible structural changes in the morphology of the gold nanoparticles can be easily justified in terms of the chronological changes in the optical response as seen through UV-Vis spectroscopy. Thus, simple addition of an external alcohol like propanol into DMF itself sequentially tweaks the longitudinal localized surface plasmon resonance (LSPR) peaks from 910nm (1.35eV, for pristine Au nanostars) to 650nm (1.87eV) in a precisely reproducible manner, as shown in figure 5a. Although the gold nanoparticle morphology tweaking have been successfully carried out by various research groups worldwide through complicated multi-step synthetic process,^{31-32, 40} our present colloidal solution synthesis stands apart among others for its inherent simplicity and ease for its reproducible quality as well as quantity.

For higher propanol concentration, gold seed particles are nucleated at a faster rate resulting in the blue shifting of LSPR with decrease in overall size of the as-formed gold nanostructures.

It is well known that the plasmon resonance of gold nanostars result from the hybridization of core and tip mode plasmons or from the near base region of the tip also.^{33, 49} Based upon this fact, we analyzed the extinction spectra of the different gold nanostructures obtained by using various DMF-propanol ratio, utilizing the standard Gaussian multi-peak fitting procedure as illustrated in figure 5c with dashed lines (fitting the optical spectra results in slight increase in intensity of longitudinal plasmon peak). The main assessment inferred from here is that the intensity of the transverse LSPR mode (corresponding to the central core) steadily grows at the expense of blue shifted longitudinal LSPR mode (related to the tips), in direct correlation with the observed HRTEM images (shown in figure 5b), strongly corroborating the fact that with increasing

propanol concentration, the tip/spike like gold nanostructures cease to grow in length, rather expands in width, customarily reducing their overall size/number. Besides, the anti-bonding plasmon mode (occurring at 800 nm in the deconvoluted optical spectra of as prepared gold nanostars) starts blue shifting with reduction in peak intensity (see Figure 5c, where the defect free single nanoparticle morphology is shown), until the MF of DMF reaches to 50, emphasizing the weakened coupling strength between the core and the tip mode plasmons, which further correlates well with the broadening as well as decrease in the overall number of tips in a single nanoparticle. But, as the MF of DMF decreases below 50, the significant anti-bonding plasmon mode appears again, depicting visually the change in the shape of the absorption spectra itself, preferably due to the inheritance of the crystal lattice defects in the nanoparticle morphology with reference to the dynamical changes in the applied synthetic procedure (see figure 5b and 5c).

Thus, the present results are in complete contrast with our earlier work involving the addition of NaOH into the DMF-PVP mixture,²⁸ which had a high impact on the reaction kinetics due to the significant oxidation of chemical inserted -OH species in between or end of the PVP polymer chain, thereby fastening the nucleation of seed particles, eventually ripening them in the form of planar elongated or spheroidal gold nanostructures; whereas mixing of DMF with an alcohol not only induces changes in the dipolar interactions within DMF, but also disrupts either partially or completely the self association of propanol, thereby allowing the essential formation of H-bonds between alcohol and the DMF. These miscible weak interactions further articulate the hydrophobic/hydrophilic end chain imbalance in PVP conformation, thus leading to the smoothening of the nucleation of seed particles, which invariably results in the congruent

size/shape tuning of the gold nanostars, as collectively summarized in the scheme 3: DMF interacts with propanol by virtue of its better hydrogen bond acceptor ability resulting in both structural as well as packing effects.

Yet, both the above mentioned synthetic protocols result in tweaking the plasmonic response (blue shifting of LSPR) which is in good correlation with their morphology but their driving forces are poles apart. In the present case of binary solvent mixture, the reaction is not dominated by kinetic parameter, easing the plausible formation of planar elongated/spheroidal gold nanostructures; while it is strongly favorable using NaOH at higher concentration (as this reaction is governed by kinetic parameter).

In tune with the literature reports supporting the fact that metal colloidal nanoparticles were able to enhance the SERS to a very large extent,^{35-39, 50-52} we have carefully analyzed the SERS data (figure 6) using the analyte, crystal violet (CV, at a concentration of 10^{-6} M) coated on the monolayer surface of our as-prepared gold nanostructures. The various enhanced Raman peaks of the dye molecule CV,^{37, 53} are tabulated with reference to their molecular origin as shown in appendix table A1.

The corresponding Raman signals of CV were greatly enhanced because lower concentrations (say, 10^{-6} M) of CV could not be detected without the assistance of a proper plasmonic substrate and enhancement factor (EF) is calculated for different samples obtained at different mole fraction of DMF (see table 1). Detailed discussion for determining the SERS EF is given in the supplementary section based upon the work of Stefania Mura et.al.⁵⁴ Assuming that all the CV molecules contribute equally, it has been demonstrated that the maximum SERS enhanced signal is obtained for pristine gold

nanostars (table 1), which first decreases (until the MF (DMF) = 33) and eventually starts increasing with higher propanol volume (table 1).

The strong enhancements observed for the central carbon atom, nitrogen atoms and π electrons in the phenyl ring of the dye molecule, crystal violet, suggest strong substrate-analyte interaction, which intrinsically depends upon two major factors: one is the surface roughness of the nanoparticles and the other is the inter-plasmon coupling-junction between two nanoparticles. Hence, in the case of pristine gold nanostars, the EM field is maximum because of its inherent surface roughness, whereas in the case pure propanol, the smaller particle size/higher surface area results in the formation of increased number of possible "hot-spots" (see figure A1). Consequently, we firmly believe that the precisely controlled nanoparticle morphology along with their structurally modified rearrangement on a substrate entrusts the responsibility of maximizing the SERS signals to large possible extent. Further work is in progress in our research group to quantitatively identify the specific role of the plasmonic substrate as well as the analyte in the SERS enhancement in terms of excitation wavelength, different analytes/concentration etc.

Conclusions

We have utilized a versatile room temperature colloidal synthesis protocol for not only the size/shape controlled anisotropic gold nanostructures, but also for precisely engineering their plasmonic response over the entire visible/NIR spectral range based on the fine tuning strategy of metal nanocrystals, which has not been possible with conventional nanocrystal growth methods or realized using existing patterning/lithographic techniques with such ease. Careful selection of the binary solvent

mixture along with the modified molecular characteristics of PVP establishes a rational paradigm in better understanding the size/shape evolution of reproducible Au nanostructure morphology, as consistently revealed through optical absorption and TEM respectively. The preliminary SERS measurements on the plasmonic substrates prepared using the air-water interfacial monolayer of the as-prepared PVP-coated Au nanostructures were systematically illustrated using the representative analyte, crystal violet.

Acknowledgements

One of the authors AK thanks CSIR for the NET-SRF fellowship. We sincerely thank the R&D Scheme, MTech (Nano) and USIC at the University of Delhi, for materials characterization. We are grateful to Mr. Rahul Bharadwaj for TEM imaging and Mr. Amit for NMR measurements.

Supporting Information

SERS spectra of pure and conjugated crystal violet on the gold nanoparticle surface along with the enhancement factor calculations are illustrated. This material is available free of charge via the Internet at <http://rsc.org>.

References

1. K. A. Willets, R. P. V. Duyne, Localized Surface Plasmon Resonance Spectroscopy and Sensing, *Annu. Rev. Phys. Chem.*, 2007, **58**, 267.
2. J. A. Schuller, E. S. Barnard, W. Cai, Y. C. Jun, J. S. White, M. L. Brongersma, Plasmonics for Extreme Light Concentration and Manipulation, *Nat. Mater.*, 2010, **9**, 193.

3. S. A. Maier, H. A. Atwater, Plasmonics: Localization and Guiding of Electromagnetic Energy in Metal/Dielectric Structures, *J. of Appl. Phys.*, 2005, **98**, 011101.
4. M. L. Brongersma, P. G. Kik, Surface Plasmon Nanophotonics, *Springer*, 2007.
5. V. Amendola, Synthesis of Gold and Silver Nanoparticles for Photonic Application, *Phd thesis, University of Padova, Italy*, 2008.
6. M. Rycenga, C. M. Cobley, W. L. Jie Zeng, C. H. Moran, D. Q. Qiang Zhang, Y. Xia, Controlling the Synthesis and Assembly of Silver Nanostructures for Plasmonic Applications, *Chem. Rev.*, 2011, **111**, 3669.
7. D. Astruc, Nanoparticles and Catalysis, *Wiley-VCHD*, 2008.
8. P. Herves, M. Perez-Lorenzo, L. M. Liz-Marzan, J. Dzubielia, Y. Lu, M. Ballauff, Catalysis by Metallic Nanoparticles in Aqueous Solution: Model Reactions, *Chem. Soc. Rev.*, 2012, **41**, 5577.
9. B. Lim, Y. Xia, Metal Nanocrystals with Highly Branched Morphologies. *Angew. Chem., Int. Ed.*, 2011, **50**, 76.
10. A. R. Tao, S. Habas, P. Yang, Shape Control of Colloidal Metal Nanocrystals, *Small*, 2008, **4**, 310.
11. M. Grzelczak, J. Perez-Juste, P. Mulvaney and L. M. Liz-Marzan, Shape Control in Gold Nanoparticle Synthesis, *Chem. Soc. Rev.*, 2008, **37**, 1783.
12. T. K. Sau and A. L. Rogach, Nonspherical, Noble Metal Nanoparticles: Colloid-Chemical Synthesis and Morphology Control, *Adv. Mater.*, 2010, **22**, 1781.
13. M. R. Langille, Chemical Methods for Controlling the Shape of Silver and Gold Nanocrystals, *Phd. Thesis, Northwestern University*, 2012.

14. Y. Xia, Y. Xiong, B. Lim, S. E. Skrabalak, Shape-Controlled Synthesis of Metal Nanocrystals: Simple Chemistry Meets Complex Physics?, *Angew. Chem. Int. Ed.*, 2009, **48**, 60.
15. J. Zhang, H. Liu, Z. Wang, N. Ming, Shape-Selective Synthesis of Gold Nanoparticles with Controlled Sizes, Shapes, and Plasmon Resonances, *Adv. Funct. Mater.*, 2007, **17**, 3295.
16. Y. Chen, X. Gu, C.-G. Nie, Z.-Y. Jiang, Z.-X. Xie, C.-J. Lin, Shape Controlled Growth of Gold Nanoparticles by a Solution Synthesis, *Chem. Commun.*, 2005, 4181.
17. A. Kedia, S. K. Pandian, Solvent-Adaptable Poly(Vinylpyrrolidone) Binding Induced Anisotropic Shape Control of Gold Nanostructures, *J. Phys. Chem. C*, 2012, **116**, 23721.
18. A. Kedia, S. K. Pandian, Precursor Driven Nucleation and Growth Kinetics of Gold Nanostars, *J. Phys. Chem. C*, 2012, **116**, 1679.
19. H. Zhang, M. Jin, Y. Xia, Noble-Metal Nanocrystals with Concave Surfaces and Their Applications, *Angew. Chem. Int. Ed.*, 2012, **51**, 7656.
20. G. Maiorano, L. Rizzello, M. A. Malvindi, S. S. Shankar, L. Martiradonna, A. Falqui, R. Cingolani, P. P. Pompa, Monodispersed and Size-Controlled Multibranched Gold Nanoparticles with Nanoscale Tuning of Surface Morphology, *Nanoscale*, 2011, **3**, 2227.
21. L. Zhao, D. Jiang, Y. Cai, X. Ji, R. Xie, W. Yang, Tuning The Size of Gold Nanoparticles in the Citrate Reduction by Chloride Ions, *Nanoscale*, 2012, **4**, 5071.

22. G. Palui, S. Ray, A. Banerjee, Synthesis of Multiple Shaped Gold Nanoparticles using Wet Chemical Method by Different Dendritic Peptides at Room Temperature, *J. Mater. Chem.*, 2009, **19**, 3457.
23. J. A. Webb, W. R. Erwin, H. F. Zarick, J. Aufrecht, H. W. Manning, M. J. Lang, C. L. Pint, R. Bardhan, Geometry-Dependent Plasmonic Tunability and Photothermal Characteristics of Multibranching Gold Nanoantennas, *J. Phys. Chem. C*, 2014, **118**, 3696.
24. M. Chirumamilla, A. Gopalakrishnan, A. Toma, R. P. Zaccaria, R. Krahne, Plasmon Resonance Tuning in Metal Nanostars for Surface Enhanced Raman Scattering, *Nanotech.*, 2014, **25**, 235303.
25. X. Xia, J. Zeng, B. McDearmon, Y. Zheng, Q. Li, Y. Xia, Silver Nanocrystals with Concave Surfaces and their Optical and Surface-Enhanced Raman Scattering Properties, *Angew. Chem. Int. Ed.*, 2011, **50**, 12542.
26. E. C. Argibay, B. Rodriguez-Gonzalez, J. Pacifico, I. Pastoriza-Santos, J. Perez-Juste, L. M. Liz-Marzan, Chemical Sharpening of Gold Nanorods: The Rod-to-Octahedron Transition, *Angew. Chem. Int. Ed.*, 2007, **119**, 9141.
27. C. M. Aguirre, Reshaping the Metallic Surface of Gold Nanoshell, *Phd. Thesis, Rice University*, 2003.
28. A. Kedia, S. K. Pandian, Controlled Reshaping and Plasmon Tuning Mechanism of Gold Nanostars, *J. Mater. Chem. C*, 2013, **1**, 4540.
29. I. Pastoriza-Santos, L. M. Liz-Marzan, N, N-Dimethylformamide as a Reaction medium for Metal Nanoparticle Synthesis, *Adv. Funct. Mater.*, 2009, **19**, 679.

30. A. V. Gaikwad, P. Verschuren, S. Kinge, G. Rothenberg, E. Eiser, Matter of Age: Growing Anisotropic Gold Nanocrystals in Organic Media, *Phys Chem Chem Phys.*, 2008, **10**, 951.
31. S. Barbosa, A. Agrawal, L. Rodri'Guez-Lorenzo, I. Pastoriza-Santos, R. A. Alvarez-Puebla, A. Kornowski, H. Weller, L. M. Liz-Marzan, Tuning Size and Sensing Properties In Colloidal Gold Nanostars, *Langmuir*, 2010, **26**, 14943.
32. C. G. Khoury, T. Vo-Dinh, Gold Nanostars for Surface-Enhanced Raman Scattering: Synthesis, Characterization and Optimization, *J. Phys. Chem. C*, 2008, **112**, 18849.
33. F. Hao, C. L. Nehl, J. H. Hafner, P. Nordlander, Plasmon Resonances of a Gold Nanostar, *Nano Lett.*, 2007, **7**, 729.
34. R. Alvarez-Puebla, L. M. Liz-Marzan, F. J. G. D. Abajo, Light Concentration at the Nanometer Scale, *J. Phys. Chem. Lett.*, 2010, **1**, 2428.
35. L. Rodri'Guez-Lorenzo, R. N. A. A. Alvarez-Puebla, F. J. G. D. Abajo, L. M. Liz-Marzan, Surface Enhanced Raman Scattering using Star-Shaped Gold Colloidal Nanoparticles, *J. Phys. Chem. C*, 2010, **114**, 7336.
36. J. Xie, Q. Zhang, J. Y. Lee, D. I. C. Wang, The Synthesis of SERS-Active Gold Nanoflower Tags for in Vivo Applications, *ACS Nano*, 2008, **2**, 2473.
37. E. N. Esenturk, A. R. H. Walker, Surface-Enhanced Raman Scattering Spectroscopy via Gold Nanostars, *J. Raman Spectro.*, 2009, **40**, 86.
38. P. R. Sajanlal, T. Pradeep, Mesoflowers: A New Class of Highly Efficient Surface-Enhanced Raman Active and Infrared-Absorbing Materials, *Nanores.*, 2009, **2**, 306.

39. B. L. Sanchez-Gaytan, P. Swanglap, T. J. Lamkin, R. J. Hickey, Z. Fakhraai, S. Link, S. J. Park, Spiky Gold Nanoshells: Synthesis and Enhanced Scattering Properties, *J. Phys. Chem. C*, 2012, **116**, 10318.
40. L. Rodríguez-Lorenzo, J. M. Romo-Herrera, J. Pérez-Juste, R. A. Alvarez-Puebla, L. M. Liz-Marzán, Reshaping and LSPR Tuning of Au Nanostars in the Presence of CTAB, *J. Mater. Chem.*, 2011, **21**, 11544.
41. S. Peng, Y. Sun, Synthesis of Silver Nanocubes in a Hydrophobic Binary Organic Solvent, *Chem. Mater.*, 2010, **22**, 6272.
42. Q. Liu, Y. Zhou, W. Tu, S. Yan, Z. Zou, Solution-Chemical Route to Generalized Synthesis of Metal Germanate Nanowires with Room-Temperature, Light-Driven Hydrogenation Activity of CO₂ into Renewable Hydrocarbon Fuels, *Inorg. Chem.*, 2014, **53**, 359.
43. K. Ramachandran, P. Sivagurunathan, K. Dharmalingam, S. C. Mehrotra, Dielectric Relaxation Study of Amide-Alcohol Mixtures by Using Time Domain Reflectometry, *Acta Phys.-Chim. Sin.*, 2007, **23**, 1508.
44. R. J. Sengwa, V. Khatri, S. Sankhla, Structure and H Bonding In Binary Mixtures of N,N- Dimethylformamide with Some Dipolar Aprotic and Aprotic Solvents By Dielectric Characterization, *Indian J. of Chem.*, 2009, **48**, 512.
45. C. Wang, H. Li, L. Zhu, S. Han, NMR and Excess Volumes Studies in DMF-Alcohol Mixtures, *J. of Solution Chem.*, 2002, **31**, 109.
46. Y. Lei, H. Li, H. Pan, S. Han, Structures and Hydrogen Bonding Analysis of N,N-Dimethylformamide and N,N-Dimethylformamide-Water Mixtures by Molecular Dynamics Simulations, *J. Phys. Chem. A*, 2003, **107**, 1574.

47. A. N. Kannappan, S. Thirumaran, R. Palani, Volumetric and Thermodynamic Studies of Molecular Interactions in Ternary Liquid Mixtures at 303, 308 and 313K. *J. of Phys. Sci.*, 2009, **20**, 97.
48. C. Hao, Y. Zhao, Y. Zhou, L. Zhou, Y. Xu, D. Wang, D. Xu, Interactions between Metal Chlorides And Poly(Vinyl Pyrrolidone) in Concentrated Solutions and Solid-State Films, *J. of Poly Sci. B: Poly. Phys.*, 2007, **45**, 1589.
49. P. Das, A. Kedia, P. S. Kumar, N. Large, T. K. Chini, Local Electron Beam Excitation and Substrate Effect on the Plasmonic Response of Single Gold Nanostars, *Nanotec.*, 2013, **24**, 405704.
50. A. J. Haes, C. L. Haynes, A. D. McFarland, G. C. Schatz, R. P. Van Duyne, S. Zou, Plasmonic Materials for Surface-Enhanced Sensing and Spectroscopy, *MRS Bulletin*, 2005, **30**, 368.
51. S. Nie, S. R. Emory, Probing Single Molecules and Single Nanoparticles by Surface-Enhanced Raman Scattering, *Science*, 1997, **275**, 1102
52. M. Fan, G. F. S. Andrade, A. G. Brolo, A Review on the Fabrication of Substrates for Surface Enhanced Raman Spectroscopy and their Applications in Analytical Chemistry, *Analytica Chimica Acta*, 2011, **693**, 7.
53. S. Yao, C. Zhou, D. Chen, Highly Porous PVA Dried Gel with Gold Nanoparticles Embedded in the Network as a Stable and Ultrasensitive SERS Substrate, *Chem. Commun.*, 2013, **49**, 6409.
54. S. Mura, G. Greppi, P. Innocenzi, M. Piccinini, C. Figus, M. L. Marongiu, C. Guob, J. Irudayaraj, Nanostructured Thin Films as Surface-Enhanced Raman Scattering Substrates, *J. Raman Spectrosc.*, 2013, **44**, 35.

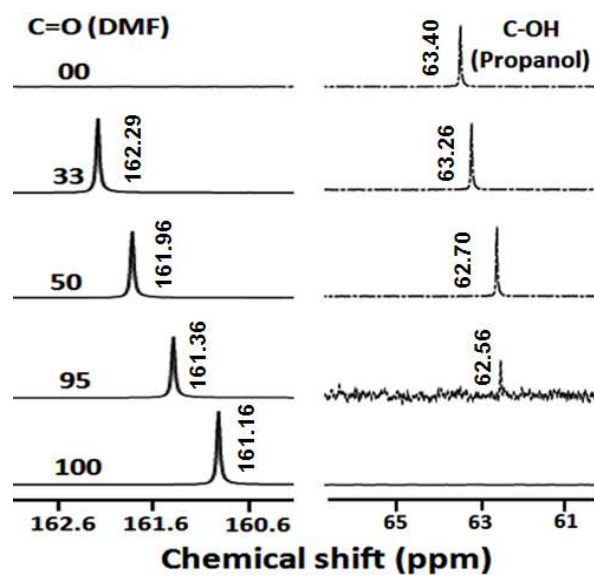
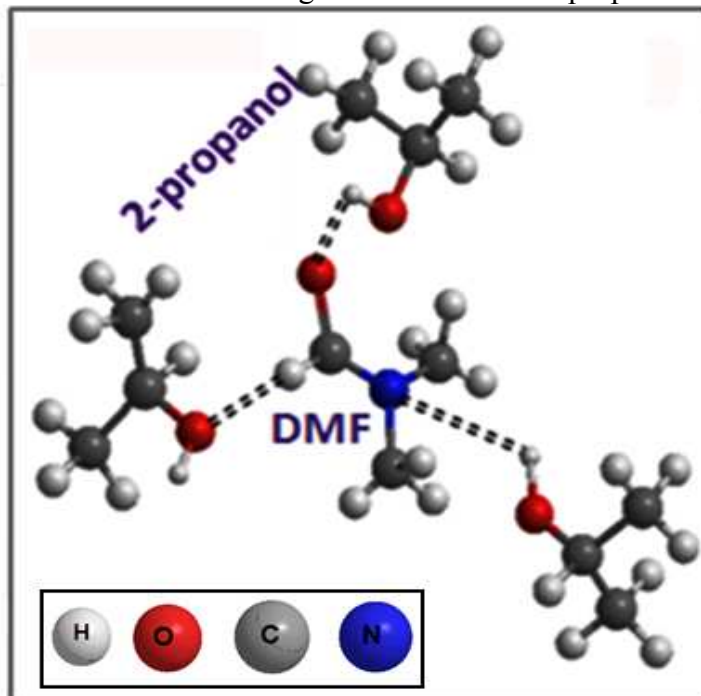


Fig 1: ^{13}C NMR spectra of DMF and DMF-propanol mixture in selective range at different MF of DMF as shown.

Scheme 1: H bonding between DMF and propanol



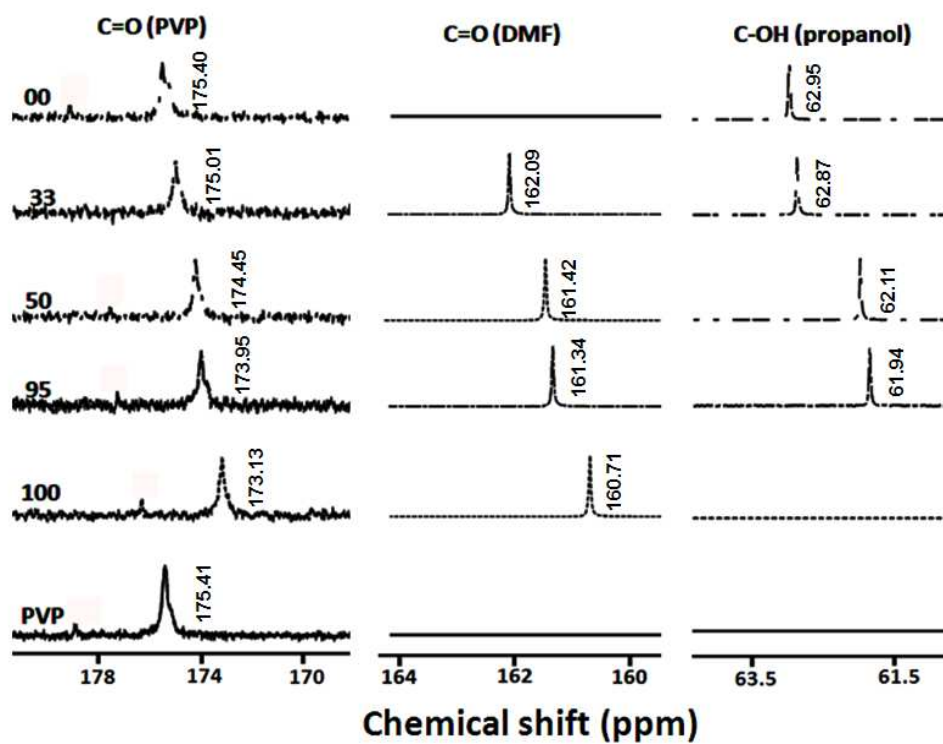
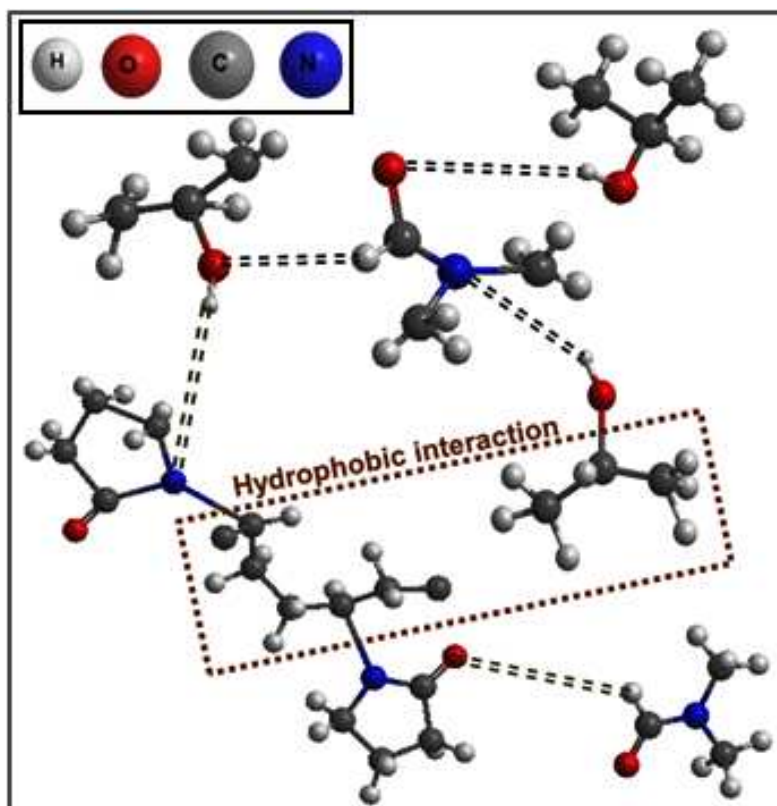


Fig 2: ^{13}C NMR spectra of PVP and PVP-DMF-propanol mixture in selective range at different MF of DMF.

Scheme 2: Interaction of PVP added to DMF-Propanol mixture.



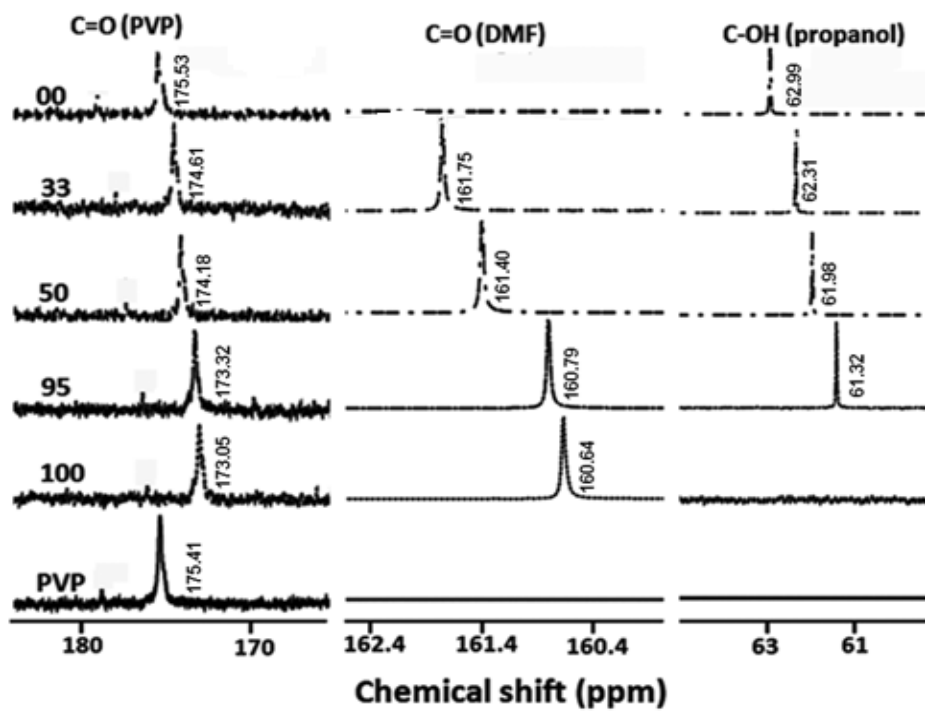


Fig 3: ^{13}C NMR spectra of PVP and Au nanoparticles in different range obtained at different MF of DMF.

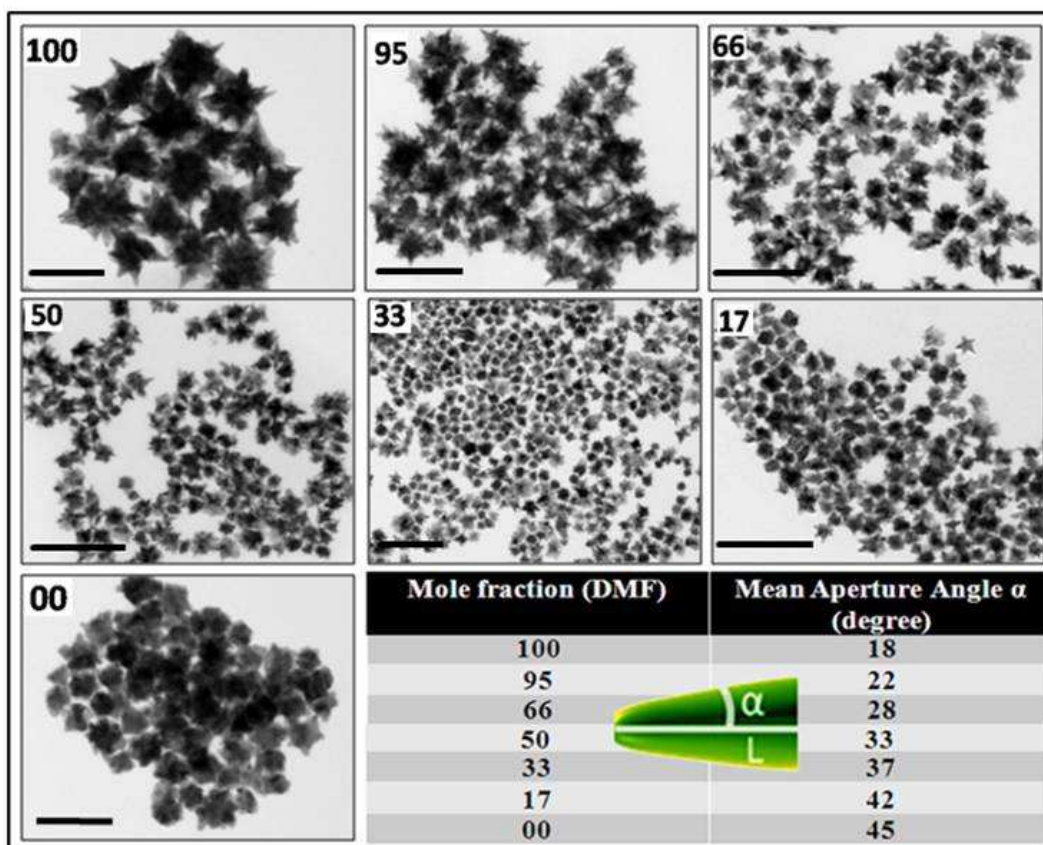


Fig 4: Morphology assessment with reference to the mean aperture angle of the as-formed anisotropic gold nanostructures with respect to increasing propanol addition in DMF (at different MF (DMF) via TEM images (scale bar =100nm).

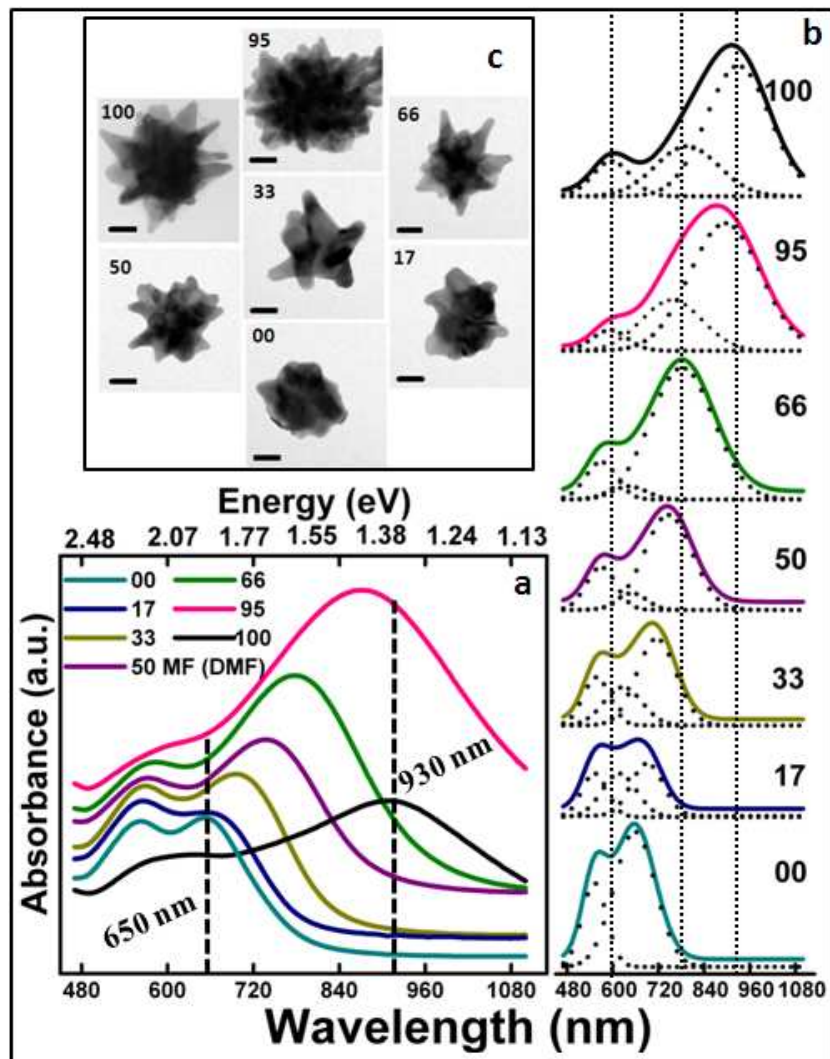
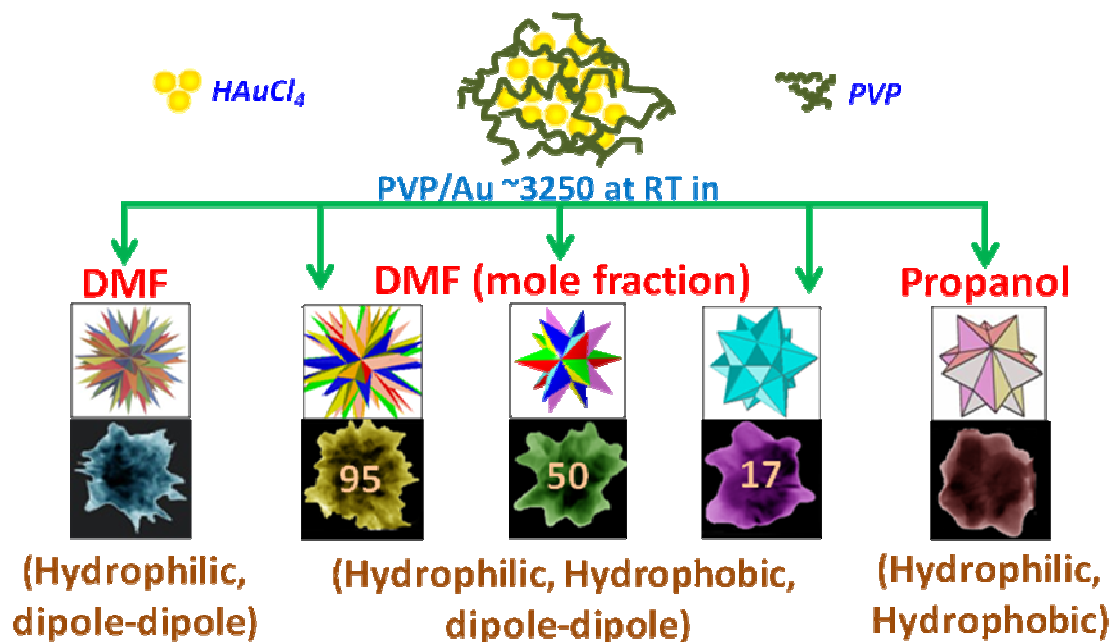


Fig 5: (a) UV-Visible absorption spectra illustrating the fine tweaking of the plasmonic signatures (from 930 nm to 650 nm) of the as-formed Au nanostructures (as shown in (b), scale bar 20 nm) with respect to different mole fraction of DMF. (c) Deconvolution of the individual plasmonic peaks correlates very well with the size/shape of the respective Au nanostructures, as discussed in detail in the text.

Scheme 3: Sequential size/shape tweaking of the gold nanostars with reference to systematic changes in the molecular interactions of PVP with the reaction mixture.



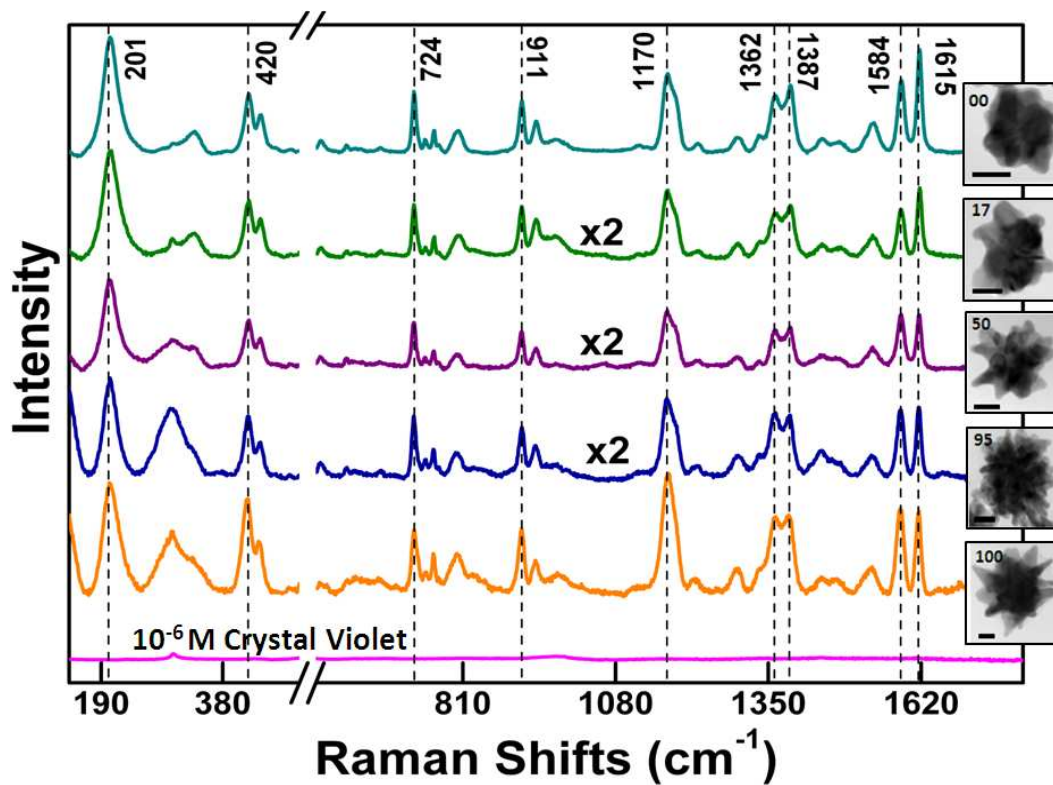


Fig 6: SERS Raman spectra of 10^{-6} M Crystal Violet without and with Au nanostructures obtained at different MF (DMF). TEM image scale bar is 20 nm

Table 1: showing the SERS enhancement factor calculated for different mole fraction of DMF which signifies the important of different size/shape of metal nanostructures.

DMF (MF)	Enhancement factor (EF)
<i>100</i>	1.90×10^4
<i>95</i>	0.60×10^4
<i>66</i>	0.34×10^4
<i>50</i>	0.43×10^4
<i>33</i>	0.31×10^4
<i>17</i>	0.50×10^4
<i>00</i>	1.20×10^4